Soils and Foundations 2015;55(3):517–528

The Japanese Geotechnical Society

Soils and Foundations

www.sciencedirect.com
journal homepage: www.elsevier.com/locate/sandf

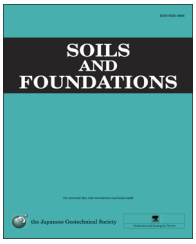

# Shear strength and dilatancy behaviour of sand–tyre chip mixtures

M.S. Mashiri[a], J.S. Vinod[a], M. Neaz Sheikh[a,*], Hing-Ho Tsang[b]

[a]School of Civil, Mining & Environmental Engineering, University of Wollongong, NSW 2522, Australia
[b]Faculty of Engineering and Industrial Sciences, Swinburne University of Technology, Hawthorn, VIC, Australia

Received 16 October 2013; received in revised form 3 December 2014; accepted 19 January 2015
Available online 7 May 2015

**Abstract**

Sand–tyre chip (STCh) mixtures can be used in many geotechnical applications as alternative backfill material. The reuse of scrap tyres in STCh mixtures can effectively address growing environmental concerns and, at the same time, provide solutions to geotechnical problems associated with low soil shear strength and high dilatancy. In this paper, the shear strength and dilatancy behaviour of STCh mixtures have been investigated. A series of monotonic triaxial tests has been carried out on sand mixed with various proportions of tyre chips. It has been found that tyre chips significantly influence the shear strength and the dilatancy behaviour of STCh mixtures. The effects of confinement and relative density on the shear strength, dilatancy and initial tangent modulus of the STCh mixtures have also been investigated. Moreover, a dilatancy model for STCh mixtures has been proposed and validated with the experimental results.


*Keywords:* Tyre; Sand–tyre chip mixture; Triaxial testing; Shear strength; Dilatancy; Initial tangent modulus

## 1. Introduction

The volume of scrap (end-of-life) tyres generated every year is increasing due to the increase in the number of vehicles worldwide. It is estimated that 1.5 billion tyres have reached their end of life every year in recent years (ETRMA, 2012). In the early 1990s, about one billion scrap tyres were stockpiled in the USA. In addition, the rate of recovery of the scrap tyres was only 11% (RMA, 2009). In the EU in 1994, the recovery rate of scrap tyres was 38% (ETRMA, 2006). A ban on the disposal of scrap tyres in landfills together with effective scrap tyre management programs have increased the scrap tyre recovery rate in many countries. At present, the recovery rate of scrap tyres has increased to 80–95% in the USA, Japan and the EU (ETRMA, 2012). Hence, scrap tyres have become an available and important secondary raw material (ETRMA, 2011), which can be effectively used in civil engineering projects. The unique properties of scrap tyres (tyre shreds or tyre chips) that are significant for civil engineering applications include low density, good insulation properties, good drainage capability, good long-term durability, high compressibility and low earth pressure. Despite the beneficial engineering properties of scrap tyres, only 7.4% of the scrap tyres in the European Union (ETRMA, 2011) in 2010 and only 7.8% of the scrap tyres in the USA (RMA, 2011) in 2011 were used in civil engineering applications. This might be because of the lack of adequate methods for the environmentally friendly recycling of scrap tyres for reuse in civil engineering applications.

The present uses of scrap tyres (tyre shreds or tyre chips) in civil engineering applications include soil reinforcement in

*Corresponding author. Tel.: +61 2 4221 3009; fax: +61 2 4221 3238.
*E-mail addresses:* msm617@uowmail.edu.au (M.S. Mashiri), vinod@uow.edu.au (J.S. Vinod), msheikh@uow.edu.au (M.N. Sheikh), htsang@swin.edu.au (H.-H. Tsang).

Peer review under responsibility of The Japanese Geotechnical Society.

http://dx.doi.org/10.1016/j.sandf.2015.04.004

**Nomenclatures**

| | |
|---|---|
| BSE | bounding shear envelope |
| $c_0$. | intercepts of shear envelopes (: $d$ (dilatancy), $b$ (bounding), CSR) |
| CSL | critical state line |
| CSR | constant stress ratio |
| CSRSE | constant stress ratio shear envelope |
| $C_u$ | uniformity coefficient |
| $C_c$ | coefficient of gradation |
| $d$ | dilatancy |
| $D$ | specimen diameter (mm) |
| $D50$ | specimen 50 mm in diameter and 100 mm in height |
| $D100$ | specimen of 100 mm in diameter and 200 mm in height |
| $d_0$ | dilatancy parameter |
| $d_1$, $d_2$, $d_3$, $d_4$ | calibration parameters for $d_b$ |
| $d_b$ | dilatancy at peak stress |
| $d\varepsilon_p^p$ | variation in plastic volumetric strain |
| $d\varepsilon_q^p$ | variation in plastic deviatoric strain |
| $D_r$ | relative density |
| DSE | dilatancy shear envelope in stress ratio–dilatancy relationship |
| $e$. | state line (: $d$ (dilatancy), $b$ (bounding), CSR) |
| $e_\Gamma$. | state line void ratio at $p'=1$ kPa (: csl (critical), $d$ (dilatancy), $b$ (bounding), CSR) |
| $e_m(\chi\%)$ | void ratio of matrix material with $\chi$% of TCh |
| $e_{max,m}$ | maximum matrix void ratio |
| $e_{max,s}$ | maximum sand void ratio |
| $e_{max,STCh}$ | maximum void ratio curve for STCh mixture at different percentages of TCh |
| $e_{max,TCh}$ | maximum TCh void ratio |
| $e_{max}$ | maximum void ratio of a given material |
| $e_{min,s}$ | minimum sand void ratio |
| $e_{min,STCh}$ | minimum void ratio curve for STCh mixture at different percentages of TCh |
| $e_{min,TCh}$ | minimum TCh void ratio |
| $e_{sm}$ | sand matrix void ratio |
| $e_{TChm}$ | TCh matrix void ratio |
| $G_{s,Sand}$ | specific gravity of sand |
| $G_{s,TCh}$ | specific gravity of TCh |
| $G_s$ | specific gravity of STCh mixture |
| ITM | initial tangent modulus |
| $L$ | tyre chip length (mm) |
| $M$. | frictional constant parameter (: $d$ (dilatancy), $b$ (bounding), CSR) |
| $M^*$. | equivalent frictional parameter (: $d$ (dilatancy), $b$ (bounding), CSR) |
| $m$ | dilatancy parameter in stress ratio–dilatancy relationship |
| $m_t$ | total mass of STCh for a given $\chi$% (kg) |
| $p'_0$ | effective mean stress (kPa) |
| $p_{at}$ | atmospheric pressure (101.3 kPa) |
| $q_0$. | intercepts $q$–$p'$ plane (: $d$ (dilatancy), $b$ (bounding), CSR) |
| STCh | sand–tyre chip |
| TCh | tyre chips |
| $V$ | volume of specimen ($m^3$) |
| $V_{pm}(\chi\%)$ | volume of particles of matrix material for $\chi$% at volume $V$ ($m^3$) |
| $V_{void}(\chi\%)$ | volume of void of mixture for $\chi$% at volume $V$ ($m^3$) |
| $W$ | width of tyre chip (mm) |
| $\gamma$ | dry unit weight (kN/$m^3$) |
| $\varepsilon$ | axial strain (%) |
| $\varepsilon_q$ | deviatoric strain (%) |
| $\varepsilon_p$ | volumetric strain (%) |
| $\eta^*$ | effective stress ratio |
| $\lambda$ | state line index (:csl (critical), $d$ (dilatancy), $b$ (bounding), CSR) |
| $\sigma'_3$ | effective confining pressure (kPa) |
| $\phi$. | shear envelope friction angle (: $d$ (dilatancy), $b$ (bounding), CSR) |
| $\chi$ | gravimetric percentage of tyre chips |
| $\psi$ | state parameter |
| $\psi^*$ | modified state parameter (: $d$ (dilatancy), $b$ (bounding)) |

road construction, ground erosion control, slope stabilization, thermal insulation, backfill for retaining walls and bridge abutments, edge drains and pipe trenches, septic system construction, light-rail construction, landfill construction and building foundations. However, pure tyre shreds or tyre chips (TCh) may be susceptible to exothermic reactions (Gacke et al., 1997; Humphrey, 1996). Moreover, the use of pure tyre shreds or pure TCh may compromise the serviceability of permanent geotechnical structures, as tyre shreds and TCh are highly compressible. Hence, research in recent years has been directed towards the use of sand–scrap tyre mixtures (Tsang et al., 2012) which are not vulnerable to exothermic reactions (Zornberg et al., 2004). Furthermore, the compressibility of sand–scrap tyre mixtures has been found to be significantly less (Bosscher et al., 1997).

The addition of scrap tyres (tyre shreds or tyre chips) to sand was found to improve the shear strength of the sand (Ahmed, 1993; Edil and Bosscher, 1994; Foose et al., 1996; Ghazavi and Sakhi, 2005; Rao and Dutta, 2006; Zornberg et al., 2004). However, the addition of tyre crumbs (granulated rubber) to sand was found to reduce the shear strength of the sand (Kawata et al., 2008; Masad et al., 1996; Sheikh et al., 2013; Youwai and Bergado, 2003), although the ductility capacity (Sheikh et al., 2010) of the mixtures has been found to be substantial (Sheikh et al., 2013). On the other hand, sand–scrap tyre mixtures were reported to have undergone large deformation without a distinct peak or failure (Ahmed, 1993; Edil and Bosscher, 1994; Kawata et al., 2008; Masad et al., 1996; Sheikh et al., 2013; Tatlisoz et al., 1998; Youwai and Bergado, 2003; Zornberg et al., 2004). In addition, sand–scrap tyre

mixtures were reported to have a low shear modulus and a high damping ratio (e.g., Anastasiadis et al., 2012; Kaneko et al., 2013a, 2013b), low liquefaction potential (Kaneko et al., 2013a, 2013b) and remarkable damping and seismic isolation properties (Kaneko et al., 2013a). Edil and Bosshcher (1994), Ahmed (1993), Kawata et al. (2008) and Zornberg et al. (2004) reported that the compaction effort showed a negligible effect on the shear strength of sand–tyre chip (STCh) mixtures. The maximum improvement in shear strength was observed for the mixture with a TCh content (gravimetric) of 39%, and the optimum density (minimum void) of the STCh mixture was observed for TCh contents (gravimetric) of 38% to 40% (Ahmed, 1993). Ahmed (1993) and Zornberg et al. (2004) observed that the behaviour of sand–tyre shred mixtures varied from sand-like to rubber-like with an increasing proportion of tyres in the mixture. The differences in the behaviour of sand–scrap tyre mixtures were further investigated in Kim and Santamarina (2008), Lee et al. (2007, 2010). By analysing the small-strain shear modulus ($G_{max}$) of the mixture, the authors identified that the mixtures exhibit a transition from a rigid to a soft granular skeleton with the proportion (%) of tyres in the mixture. The parameters that control the skeleton (behavioural zones) of the mixture were found to be dependent on the relative size of the sand and rubber particles and the proportion of tyres in the mixture. The identification of the behavioural zones (sand-like, sand–rubber and rubber-like) of sand–scrap tyre mixtures is fundamental for their use in geotechnical engineering projects. Furthermore, the efficiency of the packing influences the behaviour of the binary material with high differences in the specific gravities of the constituent materials, rather than the dry unit weight of the binary mixture (Edil and Bosscher, 1994).

In this paper, the proportions of tyre chips in STCh mixtures that control the formation of the skeleton have been determined using the matrix void ratio ($e_m$). The behaviour of STCh mixtures for different proportions of TCh, under the same effective confining pressure, relative density and strain rate, has been investigated using monotonic drained triaxial tests. Considering the importance of the dilatancy behaviour of the mixtures, a dilatancy model for STCh mixtures has also been proposed and validated with the experimental results. In the dilatancy model, the absence of the critical state in the STCh mixture at large deformations has been effectively addressed by the modification of the critical state framework to the constant stress ratio (CSR).

## 2. Materials and methodology

The scrap tyres used in this study are classified as tyre chips (TCh) according to ASTM D 6270. Tyre chips without any steel belts were cut into rectangular shapes for a uniform thickness (smaller dimension) of approximately 6 mm. The aspect ratio of the chips was 2.8 and the maximum width was 8 mm (inset (a) in Fig. 1). It is noted that the width and the thickness of the TCh were kept at less than 1/6 of the specimen diameter ($D$) to avoid the effect of sample size on the

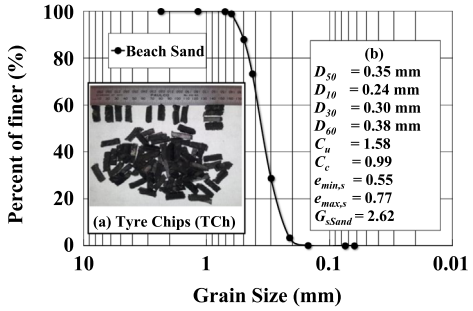


Fig. 1. Sieve analysis of beach sand used in this study—picture of tyre chips.

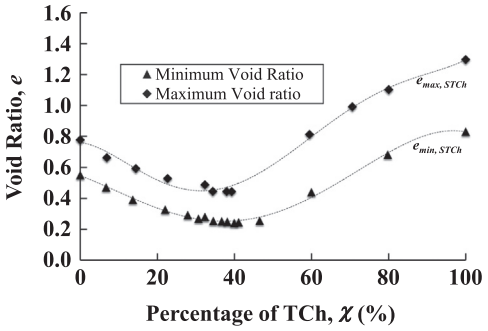


Fig. 2. Minimum and maximum void ratios of STCh mixtures for different proportions of TCh.

experimental results. The specific gravity of the TCh ($G_{s,TCh}$) was 1.12.

The particle size distribution of the sand used in this study is shown in Fig. 1. Inset (b) in Fig. 1 shows the properties of the sand. The sand is classified as poorly graded (SP). The particle size distribution of the sand is close to the sand used in Zornberg et al. (2004). Void ratios for sand, TCh and STCh mixtures were obtained according to the testing procedures in ASTM D 4253 and ASTM D 4254. However, a few additional measures were taken to achieve a homogeneous STCh mixture: (i) the sand and the TCh were premixed; and (ii) a scoop was used instead of the 13-mm funnel recommended by the Standards. It is noted that, segregations were evident for the mixture with TCh contents (gravimetric) greater than 40%. The proportions of TCh by mass, $\chi$%, in the STCh mixtures considered in this study, are 0%, 10%, 20%, 30%, 35% and 40%. The corresponding proportions of TCh by volume in the STCh mixtures are 0%, 21%, 37%, 50%, 56% and 61%, respectively. The minimum and maximum void ratios of TCh were found to be 0.83 and 1.30, respectively. The maximum and minimum void ratios of the STCh mixtures ($e_{max,STCh}$ and $e_{min,STCh}$) for different mixed proportions are shown in Fig. 2.

The $D$50 specimens (50 mm diameter × 100 mm height) for the consolidated drained (CD) monotonic triaxial tests for different mixed proportions have been prepared for dry mass $m_t$, considering the void ratio of the STCh, which is a function of the proportion of TCh. The void ratio of the mixture ($e_{STCh}$) is obtained from Fig. 2 for a desired relative density and a given proportion ($\chi$%) of TCh. The specimens were prepared using the dry deposition method in Ishihara (1996), where a

scoop was used instead of a cone-shaped funnel, due to the size of the TCh. STCh mixture samples were prepared in three layers. Every layer was compacted by carefully tamping the walls of the mould. Afterwards, the samples were saturated to a $B$-value of $>0.95$ using the back pressure saturation technique (ASTM D 7181-11). Drained shear tests were then carried out at a strain rate of 0.2%/min and no excess pore pressure developed during shearing. Additionally, a set of drained tests have been conducted on large specimens, $D100$ (100 mm diameter × 200 mm height), to check the effect of the sample size ($D50$ and $D100$) on the shear strength and dilatancy of the STCh mixture (35% TCh) at an effective confining pressure of 69 kPa and a relative density of 50%.

## 3. Experimental results

### 3.1. Void ratios

The dependence of the maximum and minimum void ratios of the STCh mixture ($e_{max,STCh}$ and $e_{min,STCh}$) on the proportion of TCh in the mixture has been shown in Fig. 2. It is important to note that the curves presented in Fig. 2 may be dependent on the properties (shape and size) of the TCh and sand. It can be observed that $e_{max,STCh}$ and $e_{min,STCh}$ initially decrease with the increase in the percentage of the TCh contents for up to 35% (by mass). Afterwards, $e_{max,STCh}$ and $e_{min,STCh}$ increase with the increase in the TCh content. The lowest values for $e_{max,STCh}$ and $e_{min,STCh}$ have been observed at 0.46 and 0.25, respectively, for the mixture with 35% of TCh (STCh (35%)). The concept of skeleton material, reported in Kim and Santamarina (2008) and Lee et al. (2007), can be used to explain the behaviour of STCh mixtures. A skeleton is formed when particles of the same material are in contact with each other and are able to transfer loads. The material forming the skeleton becomes the matrix material. The matrix void ratio ($e_m$) is defined by

$$e_m(\chi) = \frac{V_{void}(\chi)}{V_{pm}(\chi)} \quad (1)$$

where $V_{void}$ is the total volume of void in the mixture and $V_{pm}$ is the volume of particles in the matrix material.

The matrix void ratio ($e_m$) is dependent on the percentage of TCh in the STCh mixture. The feasible maximum matrix void ratio ($e_{max,m}$) is the maximum void ratio ($e_{max,m}=e_{max}$) of the individual matrix materials in the mixture. This condition enables the determination of the two percentages of TCh at which sand and rubber (tyre) stop forming the matrix material. Fig. 3 illustrates the variations in the STCh void ratio ($e_{50\%,STCh}$), the sand matrix void ratio ($e_{sm}$) and the TCh matrix void ratio ($e_{TChm}$) with the percentage of TCh for a relative density $D_r=50\%$. The intersection of the $e_{sm}$ curve with the maximum void ratio of sand ($e_{max,s}$) identifies the maximum percentage of TCh up to which sand forms the skeleton (TCh = 35%). Any increase above this percentage of TCh in the mixture will force the inter-granular voids of sand to be greater than $e_{max,s}$. Therefore, TCh becomes the matrix material forming the skeleton material of the STCh mixture, and sand fills some

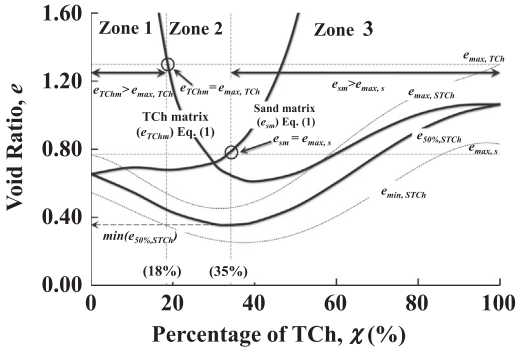


Fig. 3. Behavioural zones of STCh mixtures ($D_r=50\%$).

of the TCh voids, causing segregation. On the other hand, the interception of the $e_{TChm}$ curve with $e_{max,TCh}$ identifies the percentage of TCh in the mixture from which TCh begins forming the skeleton (TCh = 18%). Any decrease below this percentage of TCh in the STCh mixture will increase the inter-chip voids; and hence, tyre chips may not remain in contact with each other. In such a case, sand forms the skeleton and becomes the matrix material. When there are between 18% and 35% of TCh in the mixture, the skeleton is formed by both sand and TCh, such that sand and TCh collectively contribute towards the load transfer.

Based on the above analyses, two percentages of TCh have been used to define three behavioural zones that explain the mechanism of STCh mixtures (Fig. 3). This is in agreement with the observations reported in Ahmed (1993) and Zornberg et al. (2004). Zone 1 corresponds to sand-like behaviour where sand forms the skeleton (TCh < 18%). In Zone 2, sand and rubber form a binary skeleton (18% ≤ TCh ≤ 35%). Zone 3 corresponds to rubber-like behaviour where rubber forms the skeleton (TCh > 35%).

Furthermore, the minimum voids in the STCh mixture for $D_r=50\%$ and 80% have been achieved at gravimetric ratios of 35% and 40%, respectively, which are in agreement with Ahmed (1993). To fully exploit the beneficial properties of rubber, it is recommended that the STCh mixtures for use in geotechnical engineering projects should contain proportions of TCh within Zone 2. The percentages of TCh will depend of the properties of the TCh and the sand, and on the relative density of the mixture. In this study, the percentage of TCh ranges from 18% to 35% for $D_r=50\%$.

### 3.2. Effect of the proportions of TCh

Laboratory tests have been carried out for TCh amounts of 0, 10, 20, 30, 35 and 40% (by mass) at a constant relative density of 50%, an effective confining pressure of 138 kPa and an axial strain ($\varepsilon$) of approximately 35%. However, the STCh mixture specimens showed a clear shear failure plane in all the tests and did not exhibit critical state behaviour at a shear strain $\varepsilon=35\%$. Figs. 4 and 5 show the deviatoric stress versus deviatoric strain and volumetric strain versus deviatoric strain behaviours of STCh mixtures for different proportions of TCh in each mixture. The deviator stress is seen to increase with an

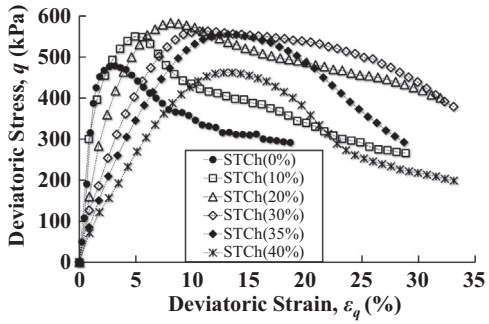


Fig. 4. Deviatoric stress-deviatoric strain behaviour of STCh mixtures ($D_r$=50%; $\sigma'_3$=138 kPa) with different proportions of TCh.

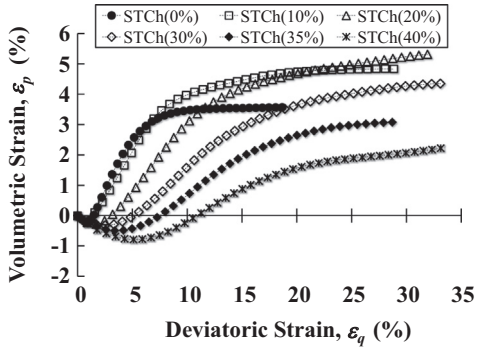


Fig. 5. Volumetric strain–deviatoric strain behaviour of STCh mixtures ($D_r$=50%; $\sigma'_3$=138 kPa) with different proportions of TCh.

increase in percentage of tyre chips up to 20%, and thereafter, to decrease slightly with the increase in tyre chips. Meanwhile, it is evident from Fig. 5 that the dilative behaviour of dense sand decreases with the inclusion of TCh. The dilative behaviour of STCh mixtures has been found to decrease with the increase in the percentage of TCh in the mixtures.

The three behavioural zones of STCh mixtures (sand-like, sand–rubber and rubber-like), mentioned previously, are evident in Figs. 4 and 5. STCh (0%) and STCh (10%) clearly show the properties of the sand-like behaviour. The inclusion of low percentages of TCh reduces the sand matrix void ratio and increases the sand matrix relative density leading to the development of higher strength, initial tangent modulus and dilatancy, as observed in the behaviour of STCh (10%) in Figs. 4 and 5. The rubber-like behaviour has been observed for STCh (40%). STCh (40%) slightly improves the shear strength of sand, but the improvement is lower than that for STCh (35%). At this percentage of TCh, the STCh mixture shows a significant reduction in the initial tangent modulus and dilatancy, which are the properties found in rubber. The sand–rubber behaviour has been observed for STCh (20%), STCh (30%) and STCh (35%). These mixtures show an improvement in the deviatoric stress and ductility capacity, the ability to sustain large deformations without failure and a reduction in the initial tangent modulus and dilatancy with the increase in percentage of TCh up to 35%, demonstrating that the skeleton is formed by both sand and rubber.

The highest amount of TCh incorporated into the sand without compromising the shear strength of the sand, but with the reduction in sand dilatancy, has been observed in STCh (35%) for the properties of TCh and sand used in this study. However, it is noted that the aspect ratio, the shape and the size of the TCh may influence the determination of the optimum percentage of tyre chips. Further research is required for correctly predicting the optimum STCh mixture for geotechnical engineering projects.

### 3.3. Effect of confining pressure ($\sigma'_3$)

Figs. 6 and 7 present the effect of the confining pressure on the shear strength and dilative behaviours of STCh (35%) in comparison with those of STCh (0%) (pure sand). Tests have been conducted for effective confining pressures of 23, 43, 69 and 138 kPa at an initial relative density of 50%. It is evident from Figs. 6 and 7 that the confining pressure has a significant influence on the shear strength and dilative behaviour of STCh mixtures. As expected, the deviator stress increases and the dilation decreases with the increase in the confining pressure (Figs. 6 and 7). Figs. 6 and 7 also compare the effect of sample size ($D$50 and $D$100) on the shear strength and dilatancy behaviour of STCh (35%) at an effective confining pressure of 69 KPa. The effect of the sample size ($D$50 and $D$100) has an insignificant influence on the peak shear strength and dilatancy of the STCh mixtures.

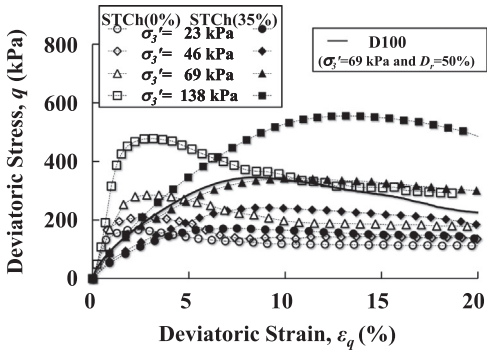


Fig. 6. Influence of effective confining pressure ($\sigma'_3$) on deviatoric stress–deviatoric strain behaviour of STCh(35%) and STCh(0%) ($D_r$=50%).

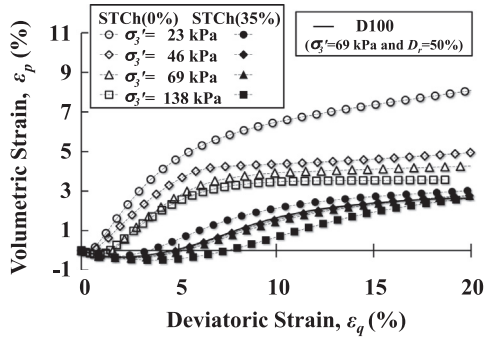


Fig. 7. Influence of effective confining pressure on volumetric strain–deviatoric strain behaviour of STCh(35%) and STCh(0%) ($D_r$=50%) .

### 3.4. Effect of relative density

Figs. 8 and 9 show comparisons of deviatoric stress versus deviatoric strain and volumetric strain versus the deviatoric strain behaviour of STCh (35%) and STCh (0%). Tests have been conducted for STCh mixtures having initial relative densities of 25%, 50% and 75% at a constant effective confining pressure of 69 kPa. It is evident from Figs. 8 and 9 that the relative density affects the shear and dilative behaviour of STCh mixtures, although to a lesser extent. Both deviatoric stress and dilation increase with an increase in the relative density of the STCh mixture. Furthermore, at all relative densities, STCh (35%) shows a greater improvement in strength and a significant reduction in the dilatancy and the initial tangent modulus compared to those of STCh (0%).

### 3.5. Initial tangent modulus (ITM)

Fig. 10 shows the initial tangent moduli (ITMs) of the STCh mixtures. It can be observed from Fig. 10 that the ITM of STCh (10%) is higher than the ITM of STCh (0%). This can be explained by the fact that with TCh contents in the mixture up to 10%, sand forms the skeleton of the matrix material, whilst the sand void ratio has been reduced by the presence of TCh (sand-like behaviour). It is observed that an increase in the TCh content beyond 18% decreases the initial tangent modulus of the mixture and this is mainly due to the active involvement of the TCh as a matrix material. The reduction in the ITM can also be due to the initial compressibility behaviour of the STCh mixture (Edil and Bosscher, 1994).

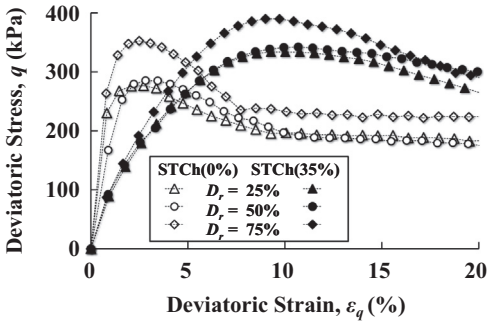


Fig. 8. Influence of relative density ($D_r$) on deviatoric stress–deviatoric strain behaviour of STCh(35%) and STCh(0%) ($\sigma'_3$ = 69 kPa).

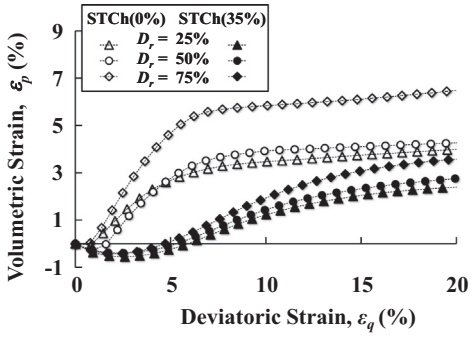


Fig. 9. Influence of relative density on volumetric strain-deviatoric strain behaviour of STCh(35%) and STCh(0%) ($\sigma'_3$ = 69 kPa).

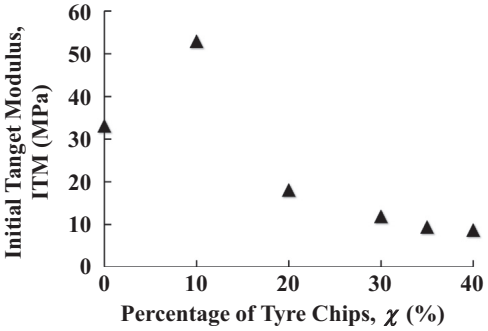


Fig. 10. Variation of initial tangent modulus (ITM) with the percentage of TCh in the STCh mixture ($D_r$ = 50%; $\sigma'_3$ = 138 kPa).

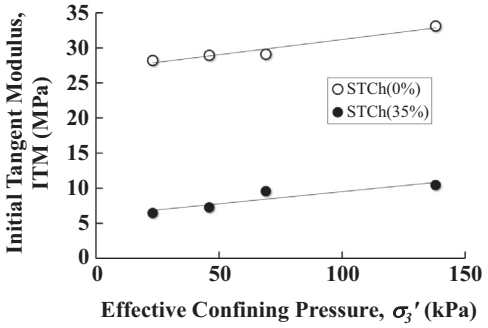


Fig. 11. Variation of initial tangent modulus (ITM) of STCh(35%) and STCh (0%) with effective confining pressure ($D_r$ = 50%).

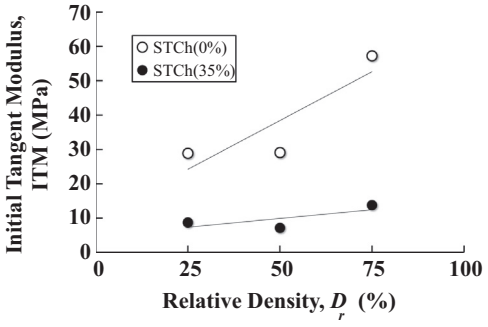


Fig. 12. Variation of initial tangent modulus (ITM) of STCh(35%) and STCh (0%) with relative density ($\sigma'_3$ = 69 kPa).

Fig. 11 shows the variation in ITM for STCh (35%) and STC (0%) with effective confining pressure. It is observed that ITM for STCh (35%) and STCh (0%) increases slightly with the effective confining pressure. As the effective confining pressure increases, the sand matrix void ratio decreases. This causes higher sand inter-particles contacts which contribute to the increase in ITM.

Fig. 12 shows the variation in ITM with the relative density of the STCh mixture. The increase in the relative density causes an increase in the ITM. The ITM of STCh (0%) is significantly higher than the ITM of STCh (35%) for the same relative density.

### 3.6. Comparison with other published results

A direct comparison with other published results may be complicated, as the results of the experimental investigation depend on a number of parameters, including specimen preparation, type of scrap tyres, size and aspect ratio of scrap tyres, confining pressure and the type of equipment used. Nevertheless, the results of this study have been compared with two previous investigations (triaxial test results) on STCh mixtures with similar gravimetric percentages of TCh under a similar effective confining pressure. The peak deviatoric stress and the volumetric strain at the peak deviatoric stress of STCh (35%) at different effective confining pressures were compared with the experimental results in Zornberg et al. (2004) and Youwai and Bergado, 2003. According to Zornberg et al. (2004), the specimens had tyre chips with an aspect ratio of 4 (Table 1). The specimens were prepared with the sand matrix (relative density of 55%) and 38% of TCh. The triaxial tests were carried out on dry specimens. On the other hand, Youwai and Bergado (2003) carried out triaxial tests on saturated specimens of sand with tyre crumbs with an aspect ratio of 1 and the specimens were prepared under dynamic compaction. The Youwai and Bergado (2003) specimens contained 30% of tyre crumbs (Table 1).

Fig. 13 shows the peak deviatoric stress and the volumetric strain at the peak deviatoric stress at different effective confining pressures. The Youwai and Bergado (2003) results show lower peak deviatoric stress mainly due to the inclusion of tyre crumbs, rather than tyre chips. Zornberg et al. (2004) show a higher value for the peak deviator stress, which can be attributed to the size of the TCh compared to the TCh used in this study. In terms of the volumetric strain at the peak deviatoric stress, the Zornberg et al. (2004) specimens show more dilative behaviour and the Youwai and Bergado (2003) specimens show less dilative behaviour than the specimens used in this study. This is mainly due to the size and the aspect ratio of the scrap tyres (Zornberg et al., 2004). Despite the differences in the scrap tyres and the test conditions, the findings of this research compare well with the findings of previous investigations.

### 3.7. Dilatancy behaviour

Fig. 14(a–c) shows the variation in the effective stress ratio ($\eta^* = q/p'$) with dilatancy $d = d\varepsilon_p^p / d\varepsilon_q^p$ for STCh mixtures in Zones 1, 2 and 3, respectively. Fig. 14a shows the dilatancy behaviour exhibited by STCh (0%) and STCh (10%). It is evident that the stress ratio increases with dilatancy irrespective of the TCh contents. In this zone, the STCh (10%) shows a higher value for $\eta^*$ with $d$ compared to that of sand. Fig. 14b shows the $\eta^* - d$ behaviour for STCh (20%), STCh (30%) and STCh (35%). These mixtures show unique values for the stress ratios ($\eta^*$) at $d=0$ and also at the peak stress ratio. However, the slope of the curves increases with the increase in the percentage of TCh contents. The STCh mixture in Zone 3 (TCh=40%) shows a similar value for the stress ratio at $d=0$ as in Zone 2. However, STCh (40%) achieves a lower peak stress ratio than that for the mixtures in Zone 2, as expected, since rubber is the only matrix material in Zone 3. It is noted that the post peak dilatancy behaviour decreases for all STCh mixtures.

Fig. 15(a–b) shows the influence of the initial effective mean stress ($p'_0$) ($p'_0 = \sigma'_3$) for STCh (0%) and STCh (35%), respectively. It is noted that the term effective mean stress, instead of effective confining pressure, has been used for modelling the dilatancy behaviour of the STCh mixtures in the following section, especially for the ease of explanation. It can be observed that the effective mean stress has a significant influence on the dilatancy behaviour of STCh mixtures. It is evident from Fig. 15(a–b) that the stress ratio and the dilatancy at the peak stress decrease with the increase in $p'_0$. It is noted that initial slope of the dilatancy curve remains constant irrespective of $p'_0$. However, the initial slope of dilatancy for STCh (35%) has been observed to be higher than that of STCh (0%) at all confining pressures. Fig. 15b clearly highlights that the inclusion of tyre chips decreases the dilatancy of sand. The post peak dilatancy has been found to be decreased at all confining pressures.

Fig. 16 presents the effect of relative density ($D_r$) on the $\eta^* - d$ behaviour for STCh (0%) and STCh (35%). It is evident that $\eta^*$ increases with the increase in $D_r$ for both STCh (0%) and STCh (35%). However, the slope of dilatancy for STCh

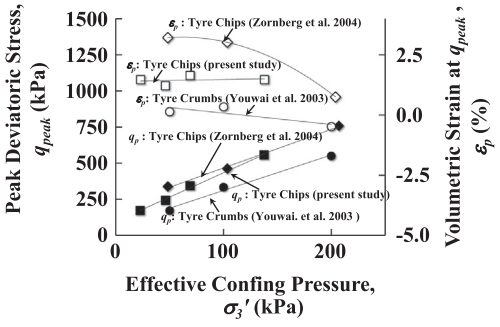


Fig. 13. Peak deviatoric stress versus Effective confining pressure and Volumetric strain at peak deviatoric strain versus Effective confining pressure for experimental data, Youwai and Bergado (2003) and Zornberg et al. (2004) (See Table 1 for properties of specimens and tests).

Table 1
Properties of the test specimen.

| Reference | $\sigma'_3$ (kPa) | Scrap tyre | Specimen | % of scrap tyre | $\gamma$(kN/m$^3$) | L Length (mm) | W Width (mm) | Aspect Ratio L/W |
|---|---|---|---|---|---|---|---|---|
| This study | 23, 46, 69 & 138 | Tyre chips | Saturated | 35 | 12.90 | 20 | 6 to 8 | 2.8 |
| Zornberg et al. (2004) | 48.3, 103.5 & 207 | Tyre chips | Dry | 38 | 15.64 | 50.8 | 12.7 | 4 |
| Youwai and Bergado (2003) | 50, 100 & 200 | Tyre crumbs | Saturated | 30 | 14.43 | $4 < L < 16$ | $4 < W < 16$ | 1 |

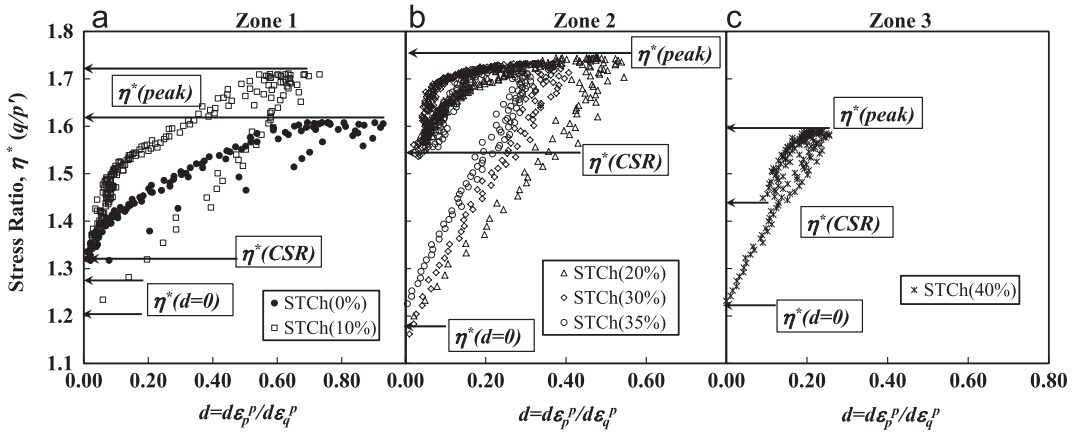


Fig. 14. Stress ratio-versus dilatancy for STCh mixtures ($D_r$=50%; $\sigma'_3$=138 kPa): (a) Zone 1: sand-like, (b) Zone 2: sand–rubber and, (c) Zone 3: rubber- like.

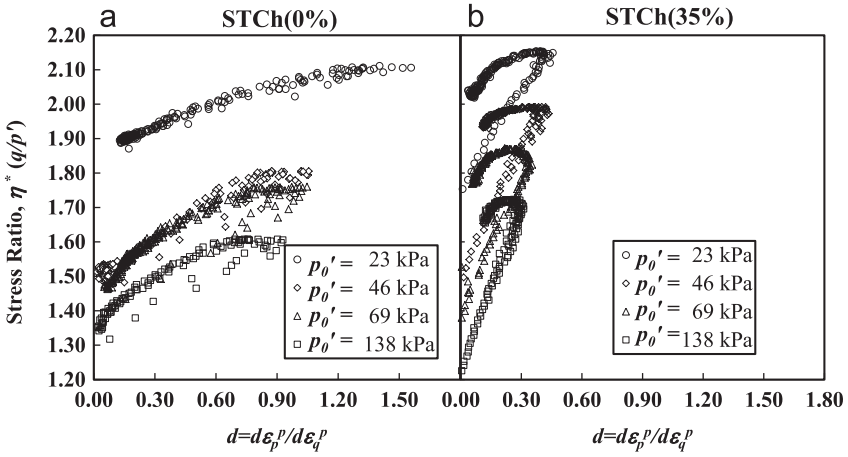


Fig. 15. Stress ratio versus dilatancy for STCh mixtures ($D_r$=50%) at different initial effective mean stresses ($p'_0$): (a) STCh(0%) and (b) STCh(35%).

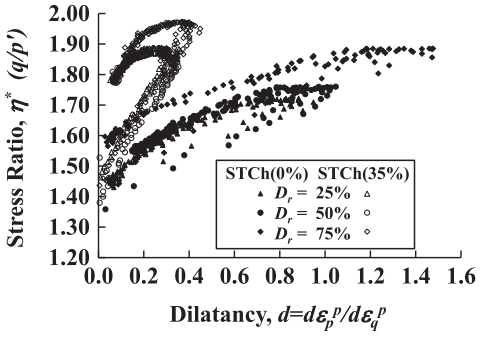


Fig. 16. Stress ratio versus dilatancy for STCh(35%) and STCh(0%) at different relative densities ($p'_0$=69 kPa).

(35%) has been observed not to have been affected by $D_r$. As expected, the dilatancy for STCh (35%) is significantly lower than that of sand. The post peak dilatancy has been found to be decreased for all $D_r$.

Dilatancy is a fundamental aspect of soil behaviour and is described by the tendency of soil to change volume during shearing (Houslby, 1991; Taheri et al., 2012). It significantly affects the behaviour of constrained soils. It has been demonstrated from the experimental investigations that the inclusion of TCh in sand (i.e., STCh mixture) controls softening and the reduction in strength after the peak and further controls the dilatancy of pure sand at all confining pressures. The improvement of the sand's shear strength and the reduction in dilatancy behaviour make STCh mixtures attractive construction materials for geotechnical engineering projects. The dilatancy behaviour of STCh mixtures has been further investigated and a dilatancy model for STCh mixtures has been developed in Section 4.

## 4. Dilatancy model for STCh mixtures

The dilatancy behaviour of STCh mixtures is influenced by the stress ratio ($\eta^*$), the percentage of tyre chips ($\chi$%), the effective mean stress ($p'_0$) and the relative density ($D_r$). Therefore, the dilatancy ($d = d\varepsilon_p^p/d\varepsilon_q^p$) can be expressed as

$$\frac{d\varepsilon_p^p}{d\varepsilon_p^q} = f(\eta^*, \chi\%, p'_0, D_r) \tag{2}$$

Li and Dafalias (2000) proposed a stress ratio-dilatancy relationship for sand as

$$d = d_0\left(\exp^{\psi m} - \frac{\eta^*}{M}\right) \tag{3}$$

where, $d_0$ and $m$ are the parameters of the soil mixture, $\psi$ is the state parameter, $M$ is the critical stress ratio and $\eta^*$ is the effective stress ratio. Youwai and Bergado (2003) applied Eq. (3) to predict the behaviour of shredded tyre-sand mixtures.

The state parameter ($\psi$), introduced by Been and Jefferies (1985), can be expressed as a function of the effective mean stress and the void ratio:

$$\psi = e - (e_{\Gamma csl} - \lambda \ln(p')) \tag{4}$$

where $e$ is the current void ratio of the material at mean stress $p'$, and $e_{\Gamma csl}$ and $\lambda_{csl}$ are parameters defining the critical state line (CSL) in the $e-p'$ plane.

It is noted that the critical state, as defined for conventional soils ($d=0$ and $d\eta^*=0$), does not occur for STCh mixtures. Youwai and Bergado (2003) described that the deformation of STCh mixtures was due to a rearrangement of the particles and the deformation of the tyre chips particles. In the present study, it has been observed that at large axial strains ($\geq 20\%$) and $d\eta^*=0$, the dilatancy significantly decreases after softening, although $d>0$. Therefore, the conventional critical state may not be obtained for STCh mixtures. This slight tendency to dilate after softening may be due to the deformation of the tyre chips in the mixture. This condition of large axial strain ($\varepsilon$) together with $d\cong 0$ and $d\eta^*=0$ will be referred to herein as the constant stress ratio (CSR).

The behaviour of the stress ratio-dilatancy curves (Fig. 14) clearly shows three stress ratios of interest, namely, $\eta^*(d=0)$, $\eta^*$(peak) and $\eta^*$(CSR). Each of these three stress ratios has been directly associated with the three conditions found in the triaxial tests results: $\eta^*(d=0)$ with $\varepsilon_p=$min ($\varepsilon_p=$volumetric strain), $\eta^*$(peak) with $q=q_{peak}$ (peak deviatoric stress) and $\eta^*$(CSR) with $\varepsilon\geq 20\%$ and $d\cong 0$ and $d\eta=0$. A shear envelope has been defined for each of these conditions (Fig. 17). Fig. 17 shows the variation in shear stress with normal stress for three shear envelopes, the dilatancy shear envelope (DSE) ($\varepsilon_p=$min), the bounding shear envelope (BSE) (peak strength) and the constant stress ratio shear envelope (CSRSE) ($\varepsilon\geq 20\%$ and $d\cong 0$ and $d\eta=0$) for STCh of 35%. It is evident from Fig. 17 that the friction angle increases from the DSE to the BSE. However, the friction angle slightly decreases for the CSRSE due to the strain-softening behaviour of STCh (35%). The three shear envelopes for STCh (35%) (i.e., DSE, BSE and CSRSE) show linearity within the range of confining pressure used in this study (23 kPa to 138 kPa). The DSE, BSE and CSRSE for STCh (35%) exhibit cohesion intercepts ($c_0$). These apparent cohesion intercepts are due to the extrapolation of the shear envelopes for low confining pressures (confining pressure below 23 kPa). The cohesion intercepts may facilitate the modelling of the STCh mixture as the nonlinearity of the shear envelopes that might be present at low confining pressures may be ignored. It is noted that Masad et al. (1996), Rao and Dutta (2006), Tatlisoz et al. (1998), Youwai and Bergado (2003) and Zornberg et al. (2004) also reported cohesion intercepts for STCh mixtures.

Three surfaces in the $q-p'$ plane, corresponding to each shear envelope, have been generated using the same concept of the frictional constant parameter $M$. The CSR surface in the $q-p'$ plane is defined by the frictional constant parameter at CSR ($M_{CSR}$). Similarly, $M_d$ is the frictional constant parameter for a dilatancy surface at $d=0$. The dilatancy surface corresponds to the transformation phase where the material changes from contractive to dilative (Li and Dafalias, 2000). The peak frictional constant parameter has been associated with bounding surface $M_b$. This surface captures the strain-hardening properties of the material. The respective frictional constants ($M_d$, $M_b$ and $M_{CSR}$) and the corresponding intercepts have been calculated according to Eqs. (5) and (6). To prevent negative stresses at low normal stresses, the introduction of a cap surface at $p'_0=0$ and $\eta^*=\eta$ (stress ratio of the stress path, $\eta=3$ for CD triaxial tests) is required.

$$M_{d,b,CSR} = \frac{6\ \sin\ \phi_{d,b,CSR}}{3-\ \sin\ \phi_{d,b,CSR}} \tag{5}$$

$$q_{0d,b,CSR} = \frac{3}{\sqrt{2}}\ c_{0d,b,CSR} \tag{6}$$

where $M_{d,b,CSR}$ is the stress ratio, $q_{0d,b,CSR}$ is the intercept in the $q-p'$ plane, $c_{0d,b,CSR}$ is the intercept in the shear envelope and $\phi_{d,b,CSR}$ is the friction angle for the dilatancy surface, the bounding surface and CSR, respectively. The three surfaces in the $q-p'$ plane are shown in Fig. 18. It is evident that each surface also has an intercept. The experimental data corresponding to the three conditions ($d=0$, peak and CSR) for STCh (35%) have also been included in Fig. 18. It is evident that the generation of the surfaces through the shear envelopes can enable the prediction of the stress ratios.

In Eq. (3), $\eta^*$ and $M$ are referred to as the origin of the $q-p'$ plane. An equivalent frictional constant ($M^*$), for each surface

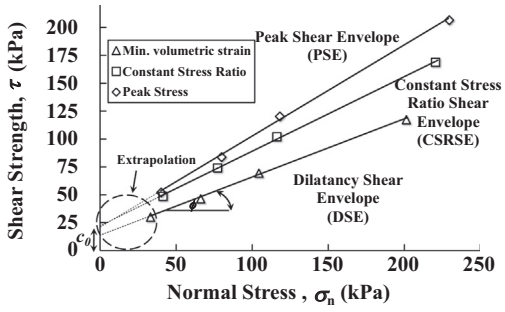


Fig. 17. Shear envelopes for STCh(35%) at minimum volumetric strain, peak deviatoric stress and constant stress ratio ($D_r=50\%$).

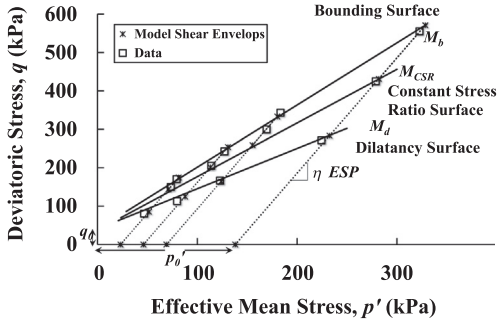


Fig. 18. Dilatancy, bounding and constant stress ratio surfaces for STCh(35%) in the $q-p'$ plane ($D_r=50\%$).

referred to as the origin of the $q-p'$ plane, has been defined in terms of $p'_0$ and $q_0$.

$$M^*_{d,b,CSR} = \frac{q_{d,b,c}}{p'_{d,b,c}} \tag{7}$$

where

$$q_{d,b,CSR} = M_{d,b,CSR} p'_{d,b,CSR} + q_0 \tag{8}$$

$$p'_{d,b,CSR} = \frac{(q_{0d,b,CSR} + \eta p'_0)}{(\eta - M_{d,b,CSR})} \tag{9}$$

and $\eta$ *is* the effective stress path ($\eta=3$ for CD triaxial tests), $M_{d,b,CSR}$ and $q_{0d,b,CSR}$ are the frictional constants and equivalent intercepts in the $q-p'$ plane.

For the three conditions previously mentioned, three state lines have been defined in the $e-p'$ plane, dilatancy state line ($e_d$), bounding state line ($e_b$) and CSR state line ($e_{CSR}$) (Fig. 19).

Each of the state lines is defined by the state line indexes $\lambda_{d,b,CSR}$ and the state line void ratios $e_{\Gamma d,b,CSR}$, STCh parameters. From Fig. 19, it can be observed that after the CSR condition has been achieved, the void ratio keeps increasing within the $e_{CSR}$. This confirms the slight tendency of the STCh mixtures to dilate after softening at large deformations. Thus, a unique CSL could not be established for the STCh mixtures (Shipton and Coop, 2012). The state parameter ($\psi$) adopted in the present study will be referred to as the constant stress state line ($e_{CSR}$) and called modified state parameter $\psi^*$.

Parameter $m$ can be calculated at the minimum volumetric strain, i.e., $d=0$, $\eta^*=M^*_d$ and $\psi^*=\psi^*_d$. Hence,

$$m = \frac{1}{\psi^*_d} \ln\left(\frac{M^*_d}{M^*_{CSR}}\right) \tag{10}$$

Dilatancy modified state parameter $\psi^*_d$ is a STCh mixture parameter given by the vertical distance between $e_{CSR}$ and $e_d$ at the effective mean stress at transformation phase $p'_d$ (Fig. 19). Since the frictional constants, $M^*_d$ and $M^*_{CSR}$, vary with $p'_0$, $m$ depends directly on initial effective mean stress $p'_0$.

Dilatancy parameter $d_0$ can be calibrated at $M^*_b$ (bounding surface) in terms of dilatancy at the peak ($d_b$), where $\eta^*=M^*_b$, $\psi^*=\psi^*_b$ and $d=d_b$. Therefore, $d_0$ can be written as

$$d_0 = \frac{d_b}{\left(e^{m\psi^*_b} - \frac{M^*_b}{M^*_{CSR}}\right)} \tag{11}$$

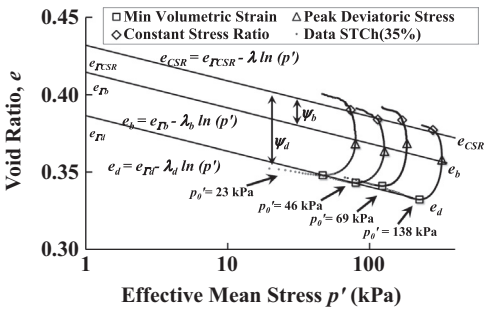


Fig. 19. Void ratio versus effective mean stress—dilatancy, bounding and constant stress ratio state lines for STCh(35%) ($D_r=50\%$).

Bounding modified state parameter $\psi^*_b$ is a STCh mixture parameter defined by the vertical distance of $e_b$ and $e_{CSR}$ at the effective mean stress at peak stress $p'_b$ (Fig. 19).

The value of $d_b$ has been found to be variable and to be inversely proportional to the initial mean stress as observed in Fig. 15b. A linear relationship has been established to define $d_b$ in terms of a normalized $p'_0$ for STCh (35%).

$$d_b = d_2 - d_1 \frac{p'_0}{p_{at}} \tag{12}$$

where $d_1$ and $d_2$ are constant calibration parameters of the STCh mixture and $p_{at}=101.3$ kPa is the atmospheric pressure. Fig. 20 shows the correlation of parameter $d_b$ with normalized initial effective stress $p'_0/p_{at}$.

The material parameters, calibration data and generated model parameters have been included in Table 2. These data can be obtained from three CD triaxial tests at different initial effective mean stresses, $p'_0$. Fig. 21 illustrates the dilatancy model prediction using Eq. (3) with $\psi^*$ and $M^*_{CSR}$ for STCh (35%) at different initial effective mean stresses. The dilatancy model clearly captures the behaviour of the STCh mixtures.

It has been observed that the values for the equivalent frictional parameters (e.g., $M^*_{CSR}, M^*_d$, and $M^*_b$) for STCh in Zone 2 and at $p'_0=138$ kPa are not influenced by the percentage of TCh in the mixture. However, the slope of the dilatancy of these STCh mixtures has been found to increase with the increase in the percentage of TCh in the mixture (Fig. 14b). It is clear that the slope of the dilatancy for these mixtures is mainly controlled by the value of $d_b$. A linear relationship has been established to define $d_b$ in terms of $\chi\%$ at $p'_0=138$ kPa.

$$d_b = f(\chi\%) = d_3 - d_4\chi \tag{13}$$

where $d_3$ and $d_4$ are calibration parameters for $10\% \le \chi\% \le 35\%$ at $p'_0=138$ kPa. Fig. 20 shows the correlation of parameter $d_b$ with the percentage of TCh at 138 kPa.

Fig. 22 shows stress ratio versus dilatancy, test results and dilatancy model predictions, for mixtures in Zone 2 at $p'_0=138$ kPa. The model parameters used to predict the behaviour of the mixtures are the ones corresponding to TCh=35%, assuming that the variations in $\psi^*_d$, and $\psi^*_b$ for mixtures in Zone 2 are not significant, except for $d_b$. The

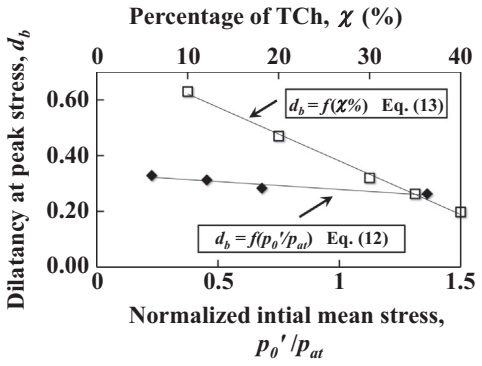


Fig. 20. Variation of dilatancy parameter $d_b$: (i) for STCh(35%) at different normalized initial mean stresses, (ii) for $p'_0=138$ kPa at different percentages of TCh.

Table 2
Parameters of dilatancy, bounding and constant stress ratio surfaces for STCh(35%) and calibration data.

| Surface | Friction angle (deg) | Frictional constant | Cohesion intercept (kPa) | $q-p'$ plane intercept (kPa) | $e_\Gamma$ at $p'=1$ (kPa) | Slope CSR | State parameter | Initial conditions | Dilatancy parameters | |
|---|---|---|---|---|---|---|---|---|---|---|
| | Tests results | Eqs. (5)–(7) | Tests results | Eq.(6) | Tests results | Tests results | Eq. (4) | | Eq. (10) | $d_b$ for STCh(35%) Eq. (12) |
| Dilatancy | $\phi_d=27.6$ | $M_d=1.09$ $M_d^*=1.33$([a]) | $c_{0d}=13.7$ | $q_{0d}=29.06$ | 0.3865 | $\lambda=0.01$ | $\psi_d=-0.0455$ | $p_0'=23$ kPa $e_0=0.3522$ | $m_{(23\ kPa)}=3.37$ | $d_1=0.057$, $d_2=0.335$ |
| Bounding | $\phi_b=39.3$ | $M_b=1.60$ $M_b^*=1.85$([a]) | $c_{0b}=20.9$ | $q_{0b}=44.33$ | 0.4155 | | $\psi_b=-0.0165$ | $p_0'=69$ kPa $e_0=0.3465$ | $m_{(69\ kPa)}=5.00$ | $d_b$ for TCh in Zone 2 at 138 kPa Eq. (13) |
| Constant stress ratio | $\phi_{CSR}=33.8$ | $M_{CSR}=1.36$ $M_{CSR}^*=1.67$ ([a]) | $c_{0CSR}=22.2$ | $q_{0CSR}=47.09$ | 0.432 | | – | $p_0'=138kPa$ $e_0=0.3390$ | $m_{(138\ kPa)}=4.98$ | $d_3=0.77$, $d_4=1.44$ |

[a] $M_d^*$, $M_b^*$ and $M_{CSR}^*$ have been calculated at $p_0'=69$ kPa.

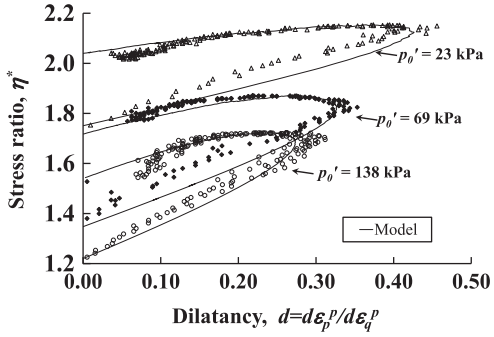


Fig. 21. Comparison of tests results and model predictions (stress ratio versus dilatancy) for STCh(35%) at different initial effective mean stresses $p_0'$ ($D_r=50\%$).

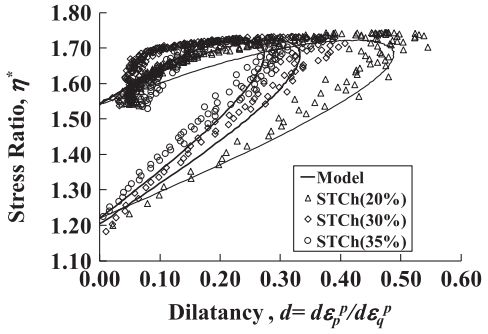


Fig. 22. Comparison of tests results and model predictions (stress ratio versus dilatancy) for STCh mixtures in Zone 2 ($p_0'=138$ kPa; $D_r=50\%$).

values for $d_b$ have been calculated from Eq. (13). It is evident that the model captures very well the dilatancy behaviour of STCh mixtures in Zone 2. As the optimum STCh mixture can be obtained in Zone 2 (sand–rubber behaviour), the dilatancy model developed herein is mainly applicable for Zone 2. Nevertheless, the dilatancy model presented can be applicable even for Zone 1 and Zone 3, if a correct set of parameters ($\phi_{d,b,CSR}$, $c_{0d,b,CSR}$, $\lambda_{d,b,CSR}$ and $e_{\Gamma d,b,CSR}$) is provided.

## 5. Summary and conclusions

This paper presents the results of triaxial tests carried out on sand–tyre chip (STCh) mixtures. The behaviour of STCh mixtures has been found to be significantly influenced by the percentage of tyre chips (TCh). Three behavioural zones (Zone 1: sand-like, Zone 2: sand–rubber and Zone 3: rubber-like) have been identified. A simple method, based on the identification of two percentages of TCh contents in the mixture, has been proposed to define the behavioural zones of STCh mixtures. Zone 1 has been defined as mixtures having sand as the matrix material, i.e., sand forms the skeleton of the mixture. Zone 2 is constituted by the binary matrix where both sand and TCh form the skeleton of the mixture. The significant improvement in shear strength and the reduction in dilatancy have been observed in Zone 2. In Zone 3, rubber forms the skeleton and the behaviour of the mixture is rubber-like. The mixture in this zone showed a similar level of sand strength albeit with a significant reduction in the dilatancy and initial tangent modulus (ITM). In this zone, the segregation of the materials has been observed as the TCh voids are not fully filled by sand.

STCh (35%) has been identified as the optimum STCh mixture for the TCh used in this study as it includes a considerable amount of TCh with a significant reduction in dilatancy and an increase in the shear strength of pure sand. It is noted that STCh (35%) is comprised of 65% of sand and 35% of TCh by mass, reducing an average 17% of the sand mass and recycling approximate 460 kg of tyres for each cubic meter of STCh mixture. The influences of confining pressure and relative density have been investigated for STCh (35%). As expected, the shear strength has been found to increase with the increase in the effective confining pressure and initial relative density. On the other hand, the dilatancy has been found to decrease with the increase in the effective confining pressure, but increase with the increase in the initial relative density of the mixture. In all cases, STCh (35%) shows improved shear strength with a significant reduction in dilatancy. ITM generally increases with the increase in the confining pressure due to increased interaction between the sand matrix and the TCh matrix. ITM has been found to increase with the increase in the initial relative density of the STCh mixture.

The dilatancy behaviour of STCh mixtures has been modelled with a modified dilatancy function introduced by Li and Dafalias (2000). The dilatancy, bounding and constant stress ratio surfaces in the $q-p'$ have been generated from the shear envelopes at three defined conditions: minimum volumetric strain, peak shear strength and constant stress ratio (CSR), respectively. The presence of cohesion, intercepting the shear envelopes, has been represented in the $q-p$ plane by the introduction of friction parameters ($M_{CSR}$, $M_d$ and $M_b$) and cohesion intercetps ($q_{0CSR}$, $q_{0d}$ and $q_0b$). Their equivalent friction parameters ($M^*_{CSR}, M^*_d$,and $M^*_b$) have been introduced to reflect the variation in these friction parameters with the initial conditions of STCh. In $e-p'$plane, the dilatancy, bounding and CSR state lines have been introduced along with modified state parameter $\psi^*$ referred to as $e_{CSR}$, instead of the CSL, for conventional soils.

Calibration parameter $d_b$ has been found to be dependent on the initial mean stress and the percentage of TCh. Two linear calibration relationships have been established to determine $d_b$. The dilatancy function predicts the behaviour of STCh mixtures well. Although the dilatancy model has been developed based on the experimental investigations of STCh (35%) in Zone 2, such a model can also be applicable for mixtures in other behavioural zones if a correct set of parameters is used.

## Acknowledgements

The work presented in this paper was supported by the University of Wollongong Small Grant 2013 and the University of Wollongong UIC International Links Grant 2011/12.

## References

Ahmed, I., 1993. Laboratory Study of Properties of Rubber-soils. Final Report, Indiana Dept. of Transp., Joint Highway Research Project. West Lafayette, Ind., Purdue University.

Anastasiadis, A., Senetakis, K., Pilitakis, K., 2012. Small-strain shear modulus and damping ratio of sand–rubber and gravel–rubber mixtures. Geotech. Geol. Eng. 30 (2), 363–382.

Been, K., Jefferies, M.G., 1985. A state parameter for sands. Geotéchnique 35 (2), 99–112.

Bosscher, P.J., Edil, T.B., Kuraoka, S., 1997. Design of highway embankments using tire chips. J. Geotech. Geoenviron. Eng. 123 (4), 295–304.

Edil, T.B., Bosscher, P.J., 1994. Engineering properties of tire chips and soil mixtures. Geotech. Test. J. 17 (4), 453.

ETRMA 2006. End of Tyre – A Valuable Resource with a Wealth of Potential – Annual Report 2006, 2 Avenue des Arts, Box 12 B-1210 Brussels, ⟨http://www.etrma.org/uploads/Modules/Documentsmanager/2006_etrma_-elts_-report.pdf⟩.

ETRMA 2011. End of Life Tyres – A Valuable Resource with Growing Potential – 2011 Edition 2 Avenue des Arts, Box 12 B-1210 Brussels, ⟨http://www.etrma.org/uploads/Modules/Documentsmanager/brochure-elt-2011-final.pdf⟩.

ETRMA 2012. Information+Enforcement=Consumer Protection—Annual Report 2011–2012, 22 August 2012, 2 Avenue des Arts, Box 12 B-1210 Brussels, ⟨http://www.etrma.org/uploads/Modules/Documentsmanager/etrma-annual-report-2012_8_def.pdf⟩.

Foose, G.J., Benson, C.H., Bosscher, P.J., 1996. Sand reinforced with shredded waste tires. J. Geotech. Eng. 122 (9), 760–767.

Gacke, S., Lee, M., Boyd, N., 1997. Field performance and mitigation of shredded tire embankment. J. Transport. Res. Board 1577 (1997), 81–89.

Ghazavi, M., Sakhi, M.A., 2005. Influence of optimized tire shreds on shear strength parameters of sand. Int. J. Geomech. 5 (1), 58–65.

Houslby G.T. 1991. How the dilatancy of soils affects their behaviour. In: Proceedings of the Tenth European Conference on Soil Mechanics and Foundation Engineering, Florence Italy, 28 May 1991, Soil Mechanics Report Number 121/91.

Humphrey, D.N. 1996. Investigation of Exothermic Reaction in Tire Shred Fill Located on SR 100 in Ilwaco, Washington. Report to the Federal Highway Administration, Washington, D.C., March 1996a, 44 p.

Ishihara, K., 1996. Soil Behaviour in Earthquake Geotechnics. Oxford University Press Inc, New York, USA.

Kaneko, K., Orense, R.P., Hyodo, M., Yoshimoto, N., 2013a. Seismic response characteristics of saturated sand deposits mixed with tire chips. J. Geotech. Geoenviron. Eng. 139 (4), 633–643.

Kaneko, T., Hyodo, M., Nakata, Y., Nyoshi, Hazarika, H., 2013b. Dynamic deformation characteristics and seismic response of tire chip and mixtures with sand. J. Jpn. Soc. Civil Eng., Ser. C (Geo. Eng.) 69 (1), 91–107.

Kawata, S., Hyodo, M., Orense, R.P., Yamada, S., Hazarika, H., 2008. Undrained and Drained Shear Behavior of Sand and Tire Chips Composite Material. International Workshop on Scrap Tire Derived Geomaterials—Opportunities and Challenges. Taylor & Francis Group, London 277–284 ISBN 978-0415-406070-5.

Kim, H.K., Santamarina, J.C., 2008. Sand–rubber mixtures (large rubber chips). Can. Geotech. J. 45 (10) 1457-1457.

Lee, C., Truong, Q.H., Lee, W., Lee, J.S., 2010. Characteristics of rubber-sand particle mixtures according to size ratio. J. Mater. Civil Eng. 22 (4), 323–331.

Lee, J.S., Dodds, J., Santamarina, J.C., 2007. Behavior of rigid-soft particle mixtures. J. Earthquake Eng. 19 (2), 179–184.

Li, X.S., Dafalias, Y.F., 2000. Dilatancy for cohesionless soils. Géotechnique 50 (4), 449–460.

Masad, E., Taha, R., Ho, C., Papagiannakis, T., 1996. Engineering properties of tire/soil mixtures as a lightweight fill material. Geotech. Test. J. 19 (3), 297–304.

Rao, G.V., Dutta, R.K., 2006. Compressibility and strength behaviour of sand–tyre chip mixtures. Geotech. Geol. Eng. 24 (3), 711–724.

RMA 2009. Scrap Tire Market in the United States. Rubber Manufacturer Association, 9th Biennial Report, May 2009, Washington DC 20005. (⟨http://www.rma.org/scrap_tires/⟩).

RMA 2011. U.S. Scrap Tire Market Summary, Feb 2013, Washington, DC 20005. (⟨http://www.rma.org/publications/scrap-tire-publications/market-reports⟩).

Sheikh, M., Mashiri, M., Vinod, J.S., Tsang, H.H., 2013. Shear and compressibility behaviours of sand–tyre crumb mixtures. J. Mater. Civil Eng. 25 (10), 1366–1374.

Sheikh, M.N, Tsang, H.H., McCarthy, T.J., Lam, N.T.K., 2010. Yield curvature for seismic design of circular reinforced concrete columns. Mag. Conc. Res. 62 (10), 741–748.

Shipton, B., Coop, M.R., 2012. On the compression behaviour of reconstituted soils. Soils Found. 52 (4), 668–681.

Taheri, A., Sasaki, Y., Tatsuoka, F., Watanabe, K., 2012. Strength and deformation characteristics of cement-mixed gravelly soil in multiple-step triaxial compression. Soils Found. 52 (1), 126–145.

Tatlisoz, N., Edil, T., Benson, C., 1998. Interaction between reinforcing geosynthetics and soil–tire chip mixtures. J. Geotech. Geoenviron. Eng. 124 (11), 1109–1119.

Tsang, H.H., Lo, S.H., Xu, X., Sheikh, M.N., 2012. Seismic isolation for low-to-medium-rise buildings using granulated rubber–soil mixtures: numerical study. Earthquake Eng. Struct. Dyn. 41 (14), 2009–2024.

Youwai, S., Bergado, D.T., 2003. Strength and deformation characteristics of shredded rubber tire–sand mixtures. Can. Geoctech. J. 40 (2), 254–264.

Zornberg, J.G., Viratjandr, C., Cabral, A.R., 2004. Behaviour of tire shred–sand mixtures. Can. Geotech. J. 41 (2), 227–241.